

# Detection of interproximal demineralized lesions on human teeth *in vitro* using frequency-domain infrared photothermal radiometry and modulated luminescence

**Raymond J. Jeon**  
**Anna Matvienko**  
**Andreas Mandelis**

University of Toronto  
Department of Mechanical and Industrial Engineering  
Center for Advanced Diffusion-Wave Technologies  
Toronto, Ontario, Canada

**Stephen H. Abrams**

Four Cell Consulting  
Toronto, Ontario, Canada

**Bennett T. Amaechi**

University of Texas Health Science Center  
at San Antonio  
Department of Community Dentistry  
Cariology Unit  
San Antonio, Texas

**Gajanan Kulkarni**

University of Toronto  
Faculty of Dentistry  
Toronto, Ontario, Canada

**Abstract.** Frequency-domain photothermal radiometry (FD-PTR or PTR) is used to detect mechanical holes and demineralized enamel in the interproximal contact area of extracted human teeth. Thirty-four teeth are used in a series of experiments. Preliminary tests to detect mechanical holes created by dental burs and 37% phosphoric acid etching for 20 s on the interproximal contact points show distinct differences in the signal. Interproximal contact areas are demineralized by using a partially saturated acidic buffer system. Each sample pair is examined with PTR before and after micromachining or treating at sequential treatment periods spanning 6 h to 30 days. Dental bitewing radiographs showed no sign of demineralized lesion even for samples treated for 30 days. Microcomputer tomography ( $\mu$ -CT), transverse microradiography (TMR), and scanning electron microscopy (SEM) analyses are performed. Although  $\mu$ -CT and TMR measured mineral losses and lesion depths, only SEM surface images showed visible signs of treatment because of the minimal extent of the demineralization. However, the PTR amplitude increased by more than 300% after 80 h of treatment. Therefore, PTR is shown to have sufficient contrast for the detection of very early interproximal demineralized lesions. The technique further exhibits excellent signal reproducibility and consistent signal changes in the presence of interproximal demineralized lesions, attributes that could lead to PTR as a reliable probe to detect early interproximal demineralization lesions. Modulated luminescence is also measured simultaneously, but it shows a lower ability than PTR to detect these interproximal demineralized lesions. © 2007 Society of Photo-Optical Instrumentation Engineers. [DOI: 10.1117/1.2750289]

**Keywords:** dental photothermal radiometry; modulated luminescence; interproximal dental caries detection; detection of demineralized dental lesions.

Paper 06184R received Jul. 5, 2006; revised manuscript received Dec. 8, 2006; accepted for publication Feb. 12, 2007; published online Jun. 28, 2007.

## 1 Introduction

The diagnosis and/or detection of dental caries or tooth decay in the early stage of its formation is a difficult and often inaccurate science. There are very few quantitative and valid methods to determine the health and integrity of tooth structure underneath the enamel surface, especially in inaccessible interproximal surfaces. Moreover, the prevalence, incidence, as well as the rate of progression of carious lesions are on the decline in fluoridated communities.<sup>1-3</sup> This reduction in smooth-surface caries has resulted in a relative increase in the incidence of small lesions in the pits and fissures and interproximal areas of teeth<sup>3</sup> as well as in the incidence of interproximal caries. These lower rates of progression make the

detection of early or incipient lesions more difficult. The detection of early demineralization or carious lesions in interproximal regions or occlusal surfaces is more difficult than readily visible smooth enamel surfaces.<sup>4</sup> To optimize medical intervention in caries treatment, an accurate assessment of the presence, extent, and activity of the lesion is fundamental. Most currently available diagnostic tools detect the lesions relatively late in the disease process when remineralization may not be possible.

The use of lasers for dental diagnostics is considered to be promising, mainly through the phenomenon of laser-induced fluorescence (or luminescence) of the enamel. The DIAGNOdent<sup>5,6</sup> is based on the fluorescence caused by porphyrins present in carious tissue and not the amount of enamel demineralization.<sup>7</sup> A number of studies were performed to as-

Address all correspondence to Andreas Mandelis, University of Toronto, 5 King's College Road, Toronto, Ontario, M5S 3G8, Canada; Tel: 1-416-978-5106; Fax: 1-416-978-5106; E-mail: mandelis@mie.utoronto.ca

sess the feasibility of using this device,<sup>8–10</sup> and it has been evaluated as having the potential to improve caries assessment in many ways. However, the original device was not designed for detection of lesions on interproximal surfaces. Eggertsson et al.<sup>11</sup> evaluated the uses of laser fluorescence (LF) and dye-enhanced laser fluorescence (DELFL) to detect early interproximal caries. They compared them to visual examination and found DELFL was better in sensitivity (the probability that a subject with the disease will have a positive test result), but DELFL and visual examination were better than LF in specificity (the probability that a subject who is free of the disease will have a negative test result). Another attempt to use quantitative light-induced fluorescence (QLF) combined with a CCD camera for detection of interproximal caries was performed, and it was found that the observed presence of interproximal lesions was dependent on camera angle, rather than on illumination angle.<sup>12</sup> Recently, a pen-type LF device, which is a portable type of DIAGNOdent with a prismatic sapphire fiber probing tip, was used by Lussi et al.<sup>13</sup> to detect approximal caries and exhibited good sensitivity (0.84 to 0.92) and specificity (0.81 to 0.93). Nevertheless, Baders and Shugars<sup>14</sup> concluded in their review that “the increased likelihood of false-positive diagnoses compared with the visual methods limits its (laser-induced fluorescence) usefulness as a principal tool.”

Since the first attempt to apply the depth profilometric capability of frequency-domain laser infrared photothermal radiometry (PTR) to the inspection of dental defects was reported by Mandelis et al.<sup>15</sup> and Nicolaidis et al.,<sup>16</sup> some of the inherent advantages of the adaptation of this technique to dental diagnostics in conjunction with modulated luminescence as a dual-probe technique have been reported.<sup>16–19</sup> The PTR technique is based on the modulated thermal IR (blackbody or Planck radiation) response of a medium, resulting from optical radiation absorption from a low-intensity laser beam ( $\sim$  milliwatts) and optical-to-thermal energy conversion followed by modulated temperature rise (“thermal waves”) usually less than 1°C in magnitude. The generated signals carry subsurface information in the form of a spatially damped temperature depth integral. In PTR applications to turbid media, such as hard dental tissue, material property and depth information are obtained in two distinct modes: conductively, from near-surface distances ( $\sim$ 5 to 500  $\mu$ m) controlled by the thermal diffusivity of enamel and the modulation frequency of the laser beam intensity; and radiatively, through mid-IR blackbody emissions from considerably deeper regions commensurate with the optical penetration of the diffusely scattered laser optical field, a diffuse photon-density wave<sup>19,20</sup> (several millimeters). The introduction of modulated (dynamic) luminescence<sup>16,20</sup> (LUM) revealed the existence of two relaxation lifetimes originating in the hydroxyapatite composition of dental enamel. Variations in LUM emission fluxes and lifetimes between healthy and carious enamel were shown to have a limited depth profilometric character.<sup>18,19</sup> A combination of PTR and LUM has been developed into an analytical caries detection tool of combined specificity and sensitivity substantially better than the DIAGNOdent, radiographic, and visual methodologies.<sup>18</sup>

The aims of the study reported in this paper are (1) to evaluate the capability of PTR and LUM to detect interproximal lesions represented by either mechanically created

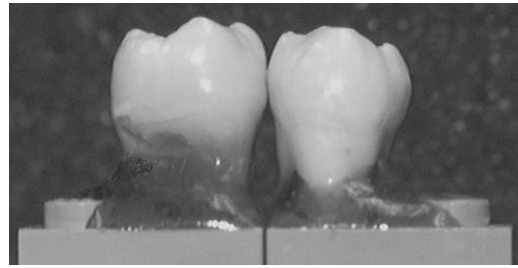


**Fig. 1** Sample pair of teeth on LEGO blocks for interproximal caries detection experiments.

$\sim$ 250- $\mu$ m-size holes, etched surfaces, or artificial demineralized lesions created by a saturated acidic buffer solution, in the interproximal contact region between two teeth; and (2) to compare the detection capabilities of PTR and LUM with established *in vitro* caries measurement and/or imaging techniques such as microcomputed tomography ( $\mu$ -CT), transverse microradiography (TMR), and scanning electron microscopy (SEM).

## 2 Materials and Methods

### 2.1 Sample Preparation

Seventeen pairs of extracted human teeth were used. Each pair was carefully cleaned with a tooth brush and polishing paste (Temrex), mounted on LEGO blocks [15.8 mm (wide)  $\times$  15.8 mm (deep)  $\times$  9.5 mm (high)], which is adapted from an idea by Buchalla et al.,<sup>12</sup> with epoxy glue (Fig. 1) and was stored in an air-tight humid container before measurements. The container consisted of two 90-mm-diam Petri dishes contacting each other rim-to-rim with a rubber band sealing off the circular contact interface. Inside this humid box, a small 35-mm-diam Petri dish was placed with distilled water to keep the ambient humidity constant. Mounting teeth on LEGO blocks enabled the teeth to be separated and remounted into the exact position during repeated measurements.

Teeth were selected with healthy mesial and distal surfaces, which had no visible defects, stains, or cracks. Since the teeth were from various human subjects, they were paired up so that intimate contact areas were created.

Each sample tooth pair was removed from the container before an experiment and was exposed to air for about 20 min for drying to avoid causing signal drift due to small humidity changes on the enamel surface. Then, the tooth was placed on the sample stage, the laser was turned on, and another 10 min lapsed before measurements commenced so that the enamel might stabilize thermally. As reported earlier,<sup>19</sup> after 20 min, the effect of hydration on optical properties such as light scattering and fluorescence as well as on thermal properties is minimal or negligible for measurements lasting less than 1 h. A long-term (3-h) test of the effect of dehydration of the surface, shown in Fig. 2, confirmed that 20 min drying in the air prior to the measurements for the case without water supply leaves the sample photothermally unaltered for up to  $\sim$ 3 h.

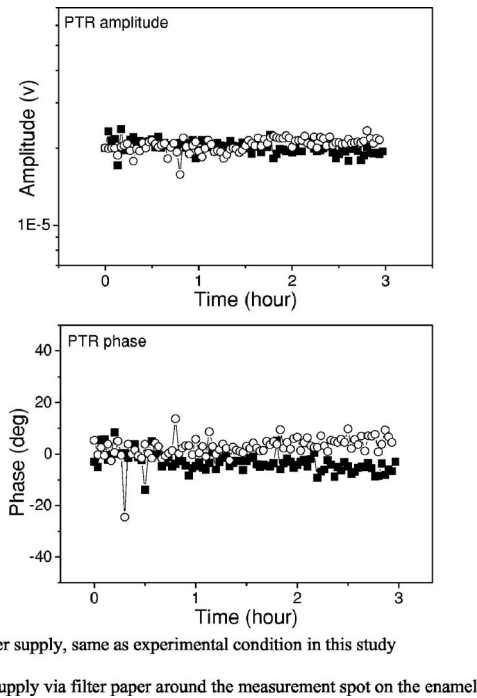


Fig. 2 Hydration effect.

### 2.2 Experimental Apparatus

Two configurations of the experimental setup were used for this study. The setup and configuration for interproximal scans (spatial scans across a contacting sample pair from either buccal or occlusal surface) is shown in Fig. 3. A semiconductor laser emitting at 670 nm (maximum power 500 mW; Sony SLD1332V) was used as the source of both PTR and LUM signals. The diameter of the laser beam was about 210  $\mu\text{m}$ . A universal diode laser driver (Coherent 6060) was used, triggered by the built-in function generator of the lock-in amplifier (Stanford Research SR830) to modulate the laser current harmonically. The modulated IR PTR signal from the tooth

was collected and focused by two off-axis paraboloidal mirrors (Melles Griot 02POA019, Rhodium coated) onto a mercury cadmium telluride (HgCdTe or MCT) detector (Judson Technologies J15D12). Before being sent to the lock-in amplifier, the PTR signal was amplified by a preamplifier (Judson Technologies PA-300). For the simultaneous measurement of PTR and LUM signals, a germanium window was placed between the paraboloidal mirrors so that wavelengths up to 1.85  $\mu\text{m}$  (Ge bandgap) would be reflected and absorbed, while IR radiation with longer wavelengths would be transmitted. The reflected modulated luminescence was focused onto a photodetector of spectral bandwidth 300 nm to 1.1  $\mu\text{m}$  (Newport 818-BB-20). A cut-on colored glass filter (Oriol 51345, cut-on wavelength: 715 nm) was placed in front of the luminescence photodetector to block laser light reflected or scattered by the tooth. To monitor the modulated luminescence, another lock-in amplifier (EG&G model 5210) was used. Both lock-in amplifiers were connected to, and controlled by, the computer via RS-232 ports.

A second set of experiments was performed to examine each of the tooth smooth surfaces involved in the interproximal contact. The two teeth were separated and frequency and line scans were performed on the individual contact areas of the tooth. The laser beam incidence was normal to the surface of the tooth involved at the contact point. This configuration was essentially similar to the one shown in Fig. 3, except the laser and the sample holder had no rotational stages and the scan involved only the individual smooth surface of the contact point. The output power of the laser (Mitsubishi ML101J27, 659 nm, maximum power 120 mW) was less than in the first configuration, as optical flux into the tooth substantially increased under normal incidence. This low-power PTR/LUM light source was adequate for normal incidence probing of the sample surface.

### 2.3 Experimental Procedures

Three kinds of experiments were performed with each sample: (1) an interproximal scan in which the laser beam scanned samples as approximal pairs at a grazing angle, cross-

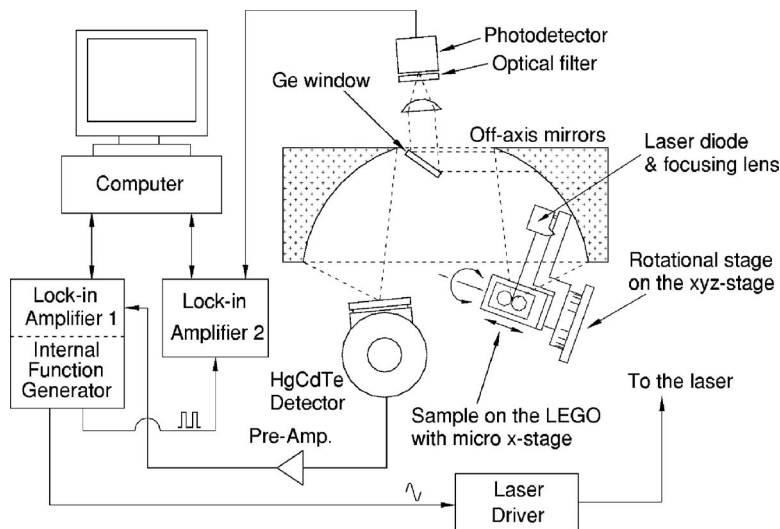


Fig. 3 Schematic diagram of PTR/LUM experimental setup.

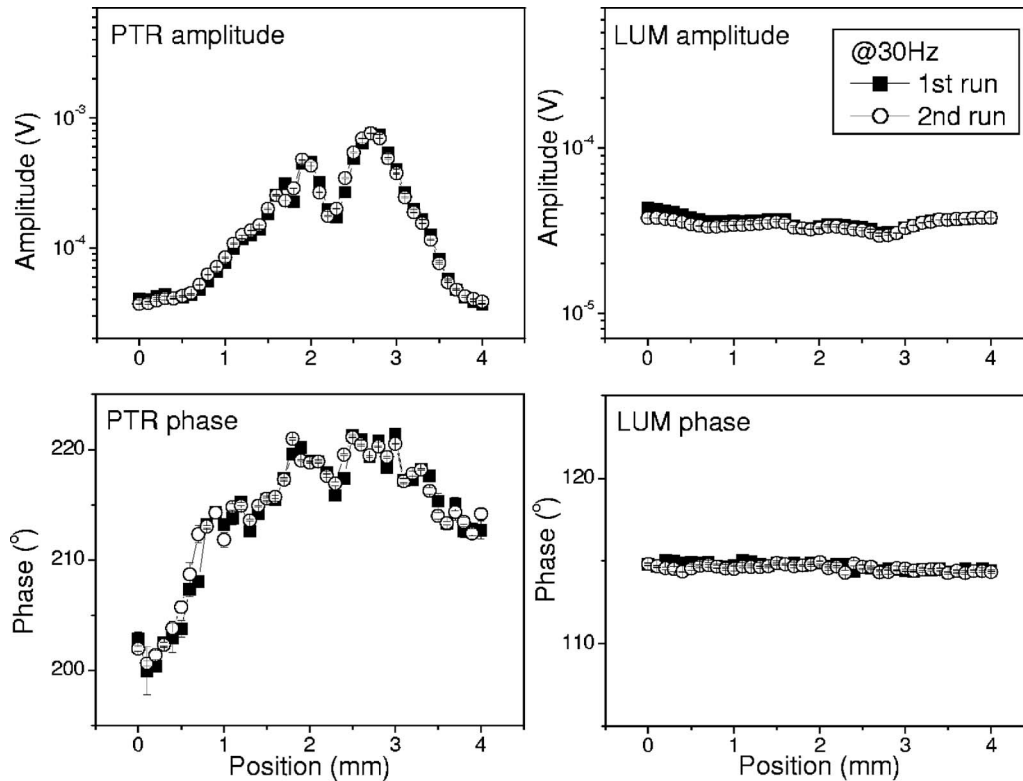


Fig. 4 Reproducibility test.

ing the contact region on either buccal or occlusal surface; (2) a line scan in which the laser scanned across the treated area of a single tooth under normal incidence; and (3) a frequency scan, which measured the PTR and LUM signals at the center of the treated area by varying the frequency from 1 Hz to 1 kHz. The frequency range was segmented into 40 equal intervals on a logarithmic scale by a data acquisition computer program and the frequency was automatically incremented to the next value after each measurement. There was a 15-s time delay between measurements at successive frequencies to allow for thermalization of the tooth surface, the latter being necessary to stabilize the signals. Regarding reproducibility, we measured a sample pair once, removed it from the stage, put it back on the stage, and measured again. The four signals (PTR amplitude and phase, LUM amplitude and phase) showed 99.92 to 100% of reproducibility (Fig. 4).

#### 2.4 Preliminary Tests

As a part of preliminary tests to assess the ability of PTR to detect interproximal lesions, two types of tests were performed. A mechanical hole was generated by 1/4-mm round carbide dental burs at the interproximal contact point of the left tooth and PTR/LUM scans across the interproximal contact area between two teeth were performed on both buccal and occlusal surfaces, as shown in Figs. 5(a) and 5(b). Subsequently, another hole was generated on the right tooth and scanned again. To test PTR/LUM sensitivity to a chemically created lesion, a 37% phosphoric acid gel in a syringe with a needle was dispensed to etch intact interproximal spots of approximately 1 mm diameter for 20 s and interproximal scans were performed in the same manner. The etching was

done while the teeth were mounted in the LEGO blocks to ensure that only the contact region was etched.

#### 2.5 Artificial Caries Lesion Detection

A partially saturated acidic buffer system<sup>21,22</sup> was used to create a demineralized lesion at the interproximal contact spots. This solution consisted of 2.2-mM potassium phosphate ( $\text{KH}_2\text{PO}_4$ ), 50-mM acetic acid ( $\text{NaOAc}$ ), 2.2-mM 1-M calcium chloride ( $\text{CaCl}_2$ ), and 0.5 ppm fluoride; the pH was adjusted to 4 to 4.5 with potassium hydroxide ( $\text{KOH}$ ). To treat only the interproximal contact areas a small drop of the solution was applied between two tooth surfaces inside the air-tight humid container, held in place by surface tension. Treated areas were about 3 mm in diameter. The interproximal solution was refreshed three times per day during the entire treatment period. Before the onset of treatments and after each sequential treatment period from 6 h to 30 days, interproximal scans, line scans, and frequency scans were performed. Dental bitewing radiographs were also taken to determine whether x-rays could identify these demineralized lesions. The radiographs were mounted perpendicular to the contact, much as would be done with a clinical bitewing radiograph.

#### 2.6 $\mu$ -CT and TMR

After completing all the experiments,  $\mu$ -CT, TMR, and SEM analyses were performed to compare and correlate the PTR signals to depth of lesions and density changes. A  $\mu$ -CT 40 from Scanco (Skyscan 1072, Scanco, USA), which enables a spatial resolution of 6  $\mu\text{m}$ , was used. The system consists of

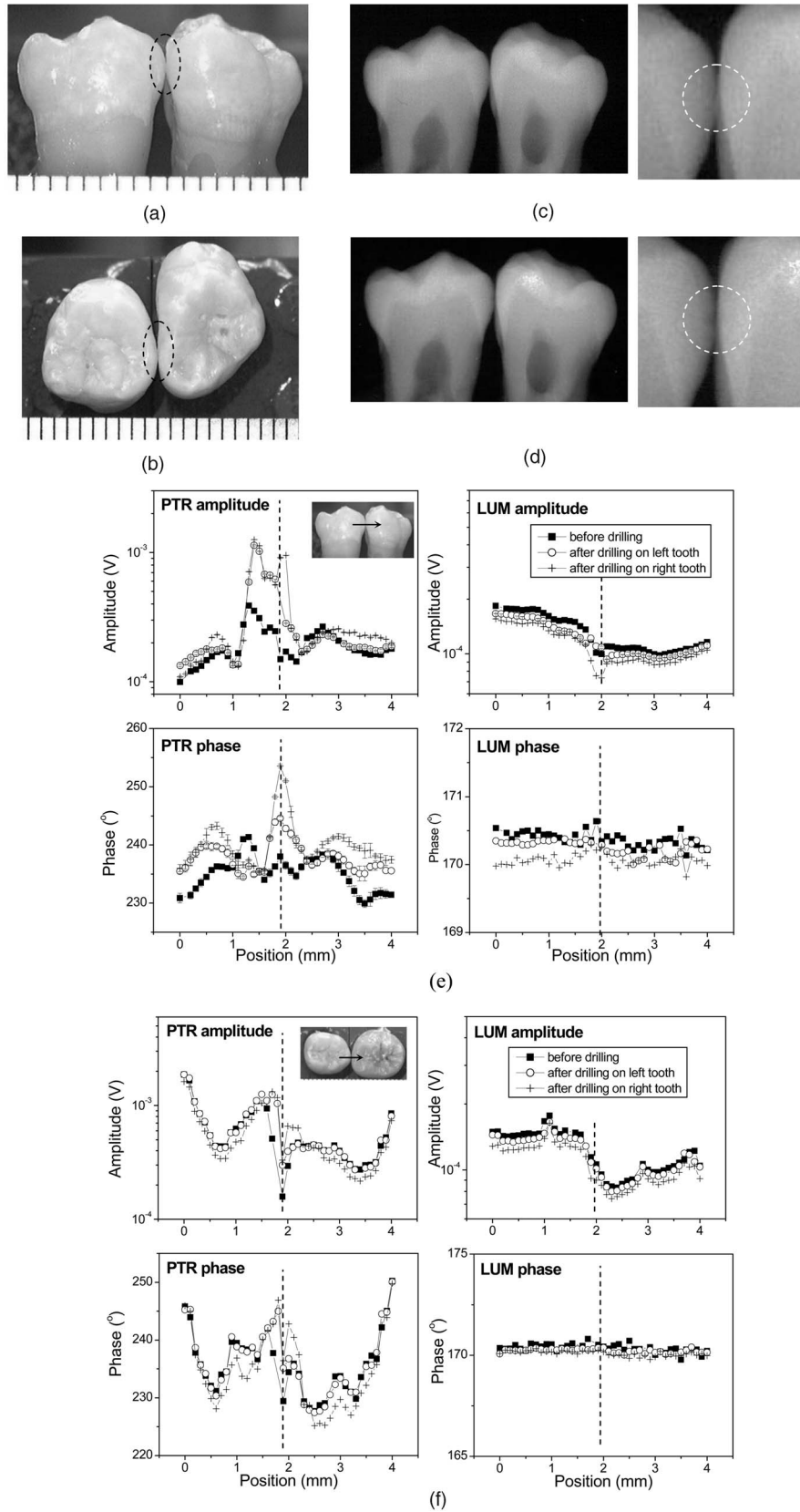


**Fig. 5** Interproximal pair of teeth with micromechanical holes: (a) side view and (b) top view of the tooth pair, (c) radiograph of the tooth pair before drilling holes and a magnified view of the contact spot on the right, (d) radiograph of the tooth pair after drilling holes in both contact spots and a magnified view of the contact spot on the right, (e) interproximal PTR/LUM scan results on the buccal surfaces at 5 Hz, and (f) interproximal scan results on the occlusal surfaces at 5 Hz.

a combination of an x-ray shadow microscope system (micro-focus x-ray tube with a high-voltage power supply and a specimen stage with a precision manipulator) and a 2-D x-ray CCD camera connected to a frame-grabber and a dual Pentium computer with color monitor and tomographic reconstruction software, V works™ 4.0 (CyberMed, Korea). Because the samples were scanned at the highest resolution of 6  $\mu\text{m}$ , which requires a narrow tube, the areas of interest were cut out as an enamel block to fit into the tube, and the samples were stabilized inside the tube using spongy foams to prevent movement during scanning. Samples were scanned at 150 kV/100  $\mu\text{A}$  and focus spot of 5  $\mu\text{m}$ , with the scanning line placed at the middle of the lesion to produce five representative tomographic images per sample. Using the density-measuring program, V works™ 4.0 (CyberMed, Korea) software, in 2-D analyzing mode, the linear attenuation coefficient (LAC,  $\text{cm}^{-1}$ ) of (1) the demineralized area and (2) the adjacent sound enamel (protected from demineralization as a control), were measured from the tomographic image of each sample to determine the mineral concentration, as described by Dowker et al.<sup>23</sup> Because the lesions that were produced had characteristics of eroded lesions (i.e., a crater and a certain depth of demineralization at the base of the lesion), the LAC was measured only within the demineralization at the base of the lesion (and not in the crater area). The value for the mineral concentration of the demineralized area or the sound area for each sample was an average of the values from the five representative images produced from each sample. The mineral loss for each sample was calculated as the difference in mineral concentration between the sound and the demineralized area.

Following  $\mu\text{-CT}$  imaging, the teeth were carefully sectioned, using a water-cooled diamond-coated wire saw (model 3242 Well, Le Locle, Switzerland) to produce an enamel slice of approximately 100  $\mu\text{m}$  thick from each lesion. These slices, together with an aluminum step wedge (10 steps of 24.5  $\mu\text{m}$  thickness), were microradiographed on type 1A high-resolution glass x-ray plates (Imtech, California, USA) with a Phillips x-ray generator system equipped with a nickel filtered  $\text{Cu-K}\alpha$  target, producing monochromatic radiation of wavelength appropriate for hydroxyapatite (184  $\text{\AA}$ ). The plates were exposed for 10 min at 20 kV/10 mA, and processed. Processing consists of a 5-min development in Kodak HR developer and 15-min fixation in Kodak Rapid-fixer before a final 30-min wash period. After drying, the microradiographs were visualized using a Leica DMR optical microscope linked via a Sony model XC-75CE closed-circuit TV (CCTV) camera to a 90-MHz Dell™ Pentium personal computer. The enhanced image of the microradiograph was analyzed under standard conditions of light intensity and magnification, and was processed, along with data from the image of the step wedge, using the TMR software<sup>24</sup> (TMRW version 2.0.27.2, Inspektor Research Inc., Amsterdam, Netherlands) to quantify the lesion parameters of integrated mineral loss ( $\Delta z$ ,  $\text{vol}\% / \mu\text{m}$ ) and lesion depth (LD, in micrometers). As stated, due to the fact that the lesions that were produced have characteristics of eroded lesions (i.e., a crater and certain depth of demineralization at the base of the lesion), the mineral loss and lesion depth was quantified as described by Amaechi et al.<sup>25</sup> for eroded lesions. The lesion depth consisted of the

depth of the crater plus the depth of the demineralization at the base of the lesion, while the mineral loss consisted of the mineral lost by both crater formation and the demineralization at the base of the lesion.

### 3 Results and Discussion

The signal-to-noise ratios (SNRs) for the PTR and the LUM signals were found to be usually in the range of tens to hundreds and hundreds to thousands, respectively. Therefore, most of the error bars shown in the figures are smaller than the size of the symbols. Some error bars were removed from some plots to improve the viewing of small signal differences between adjacent curves, if the presence of error bars was deemed as obscuring such differences.

#### 3.1 Mechanical Hole Detection

Interproximal PTR/LUM scan results on buccal and occlusal surfaces of the mechanically drilled samples are shown in Figs. 5(e) and 5(f). The black square symbols show scans at 5 Hz before machining. After making a 1/4-mm-diam and 1/4-mm-deep hole in the left tooth, PTR amplitude and phase clearly increased around the interproximal area (1.3 to 2.5 mm). After drilling a hole in the right tooth, the PTR amplitude increased again and the phase exhibited even larger changes. LUM amplitude and phase showed a slight decrease across the entire scanned length, and comparatively small changes were observed in the drilled region. Changes observed in PTR and LUM signals beyond the drilled region were likely due to increases in the density of mechanical defects (microcracks) following the drilling process. This is probably the source of baseline changes in the PTR amplitude and phase signals, whereas the LUM scans may also have been affected by the state of hydration of the enamel surface. Overall, the smooth or buccal surface scans [Fig. 5(e)] exhibited higher contrast to the presence of the interproximal mechanical defects than the occlusal surface scans [Fig. 5(f)]. Radiographs from the buccal surface were taken before and after the drilling of holes [Figs. 5(c) and 5(d), respectively]. Only the left hole is dimly visible in the magnified view in Fig. 5(d) as well as under conventional viewing conditions on a light table using magnification.

#### 3.2 Detection of Enamel Surface Etching

Figures 6(a) and 6(b) show a pair of teeth in contact. The contact areas were etched with 37% phosphoric acid gel for 20 s. Interproximal scan results on buccal and occlusal surfaces at 30 Hz in Figs. 6(d) and 6(e) show a slight decrease of the PTR amplitude in the vicinity of the etched interproximal spots. PTR amplitudes and phases on the buccal surface scans in Fig. 6(d) decreased around the etched region, while the occlusal surface scans in Fig. 6(e) did not show clear differences. The postetch radiograph in Fig. 6(c) shows no sign of the demineralized enamel surface.

#### 3.3 Artificial Demineralized Lesion Detection by PTR and LUM

Five pairs of teeth in contact were treated with the saturated buffer solution as already described. All 10 teeth were treated from 16 h to 30 days in intervals of 16, 80, 100, and 170 h, and 10, 20, and 30 days, sequentially. After each treatment

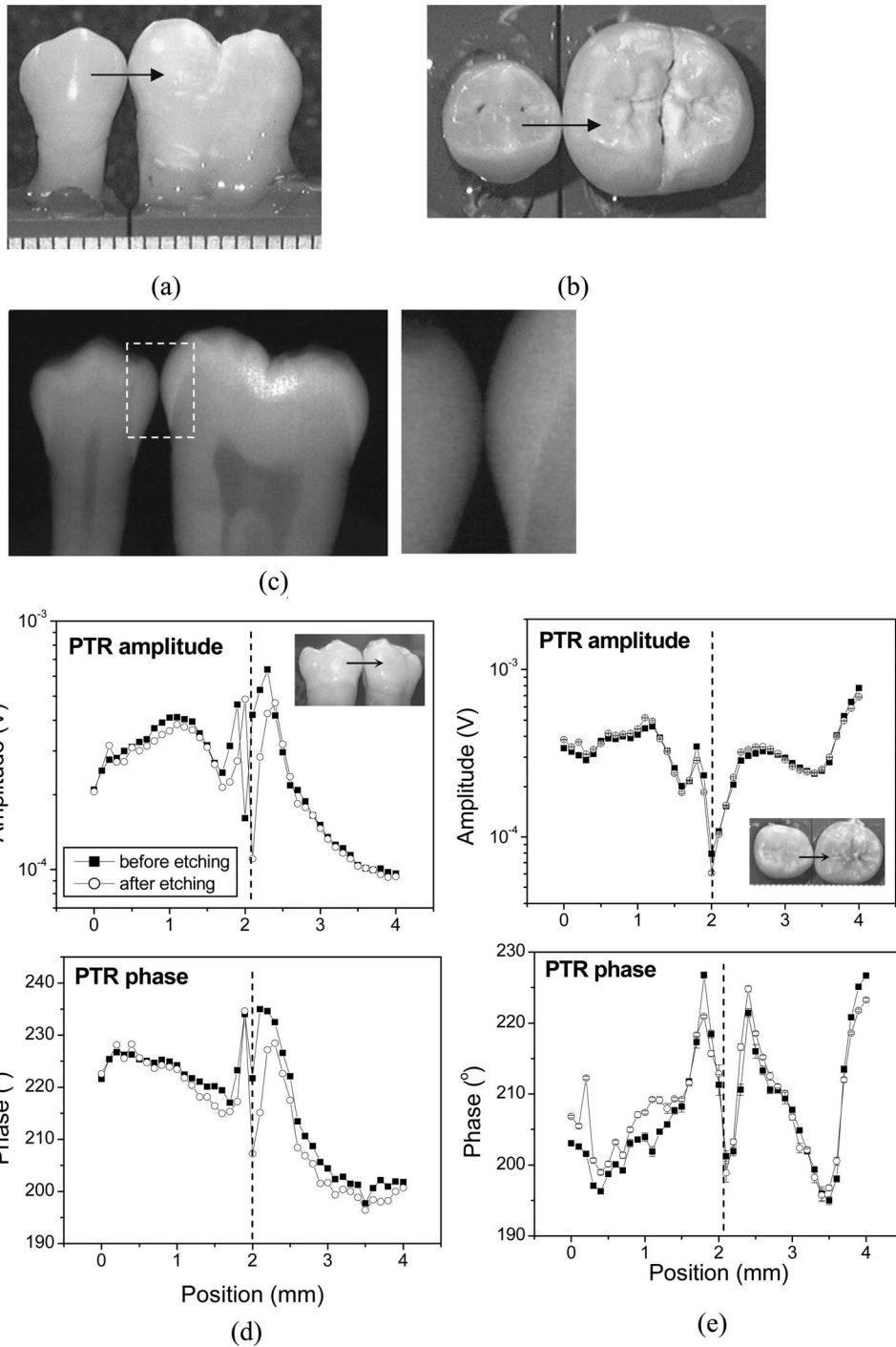


**Fig. 6** Interproximal pair of teeth with surface etching: (a) side view and (b) top view of the tooth pair, (c) radiograph of the tooth pair after etching the contact spots for 30 s and a magnified view, (d) interproximal scan results on the buccal surfaces at 30 Hz, and (e) interproximal scan results on the occlusal surfaces at 30 Hz.

period, interproximal scans at 30 Hz, line scans at 30 Hz and frequency scans from 1 to 1000 Hz were performed. Photographs of one of the sample pairs are shown in Figs. 7(a) and 7(b). Figures 7(e) and 7(f) show typical PTR and LUM responses for interproximal scans on the buccal and occlusal surface, respectively. Although measurements were performed after each treatment period, only three representative data sets, before treatment, after 16 h, and after 30 days, are shown

in the plots for clarity. After the first 16-h treatment, PTR amplitude and phase increased almost an order of magnitude in the vicinity of the interproximal area, even though the laser incidence angle near the interproximal region was grazing, almost parallel to the approximal interface. However, LUM showed almost no change around the treated contact point. Slight rigid signal amplitude decreases across the entire scanned region were observed, presumably due to dehydration

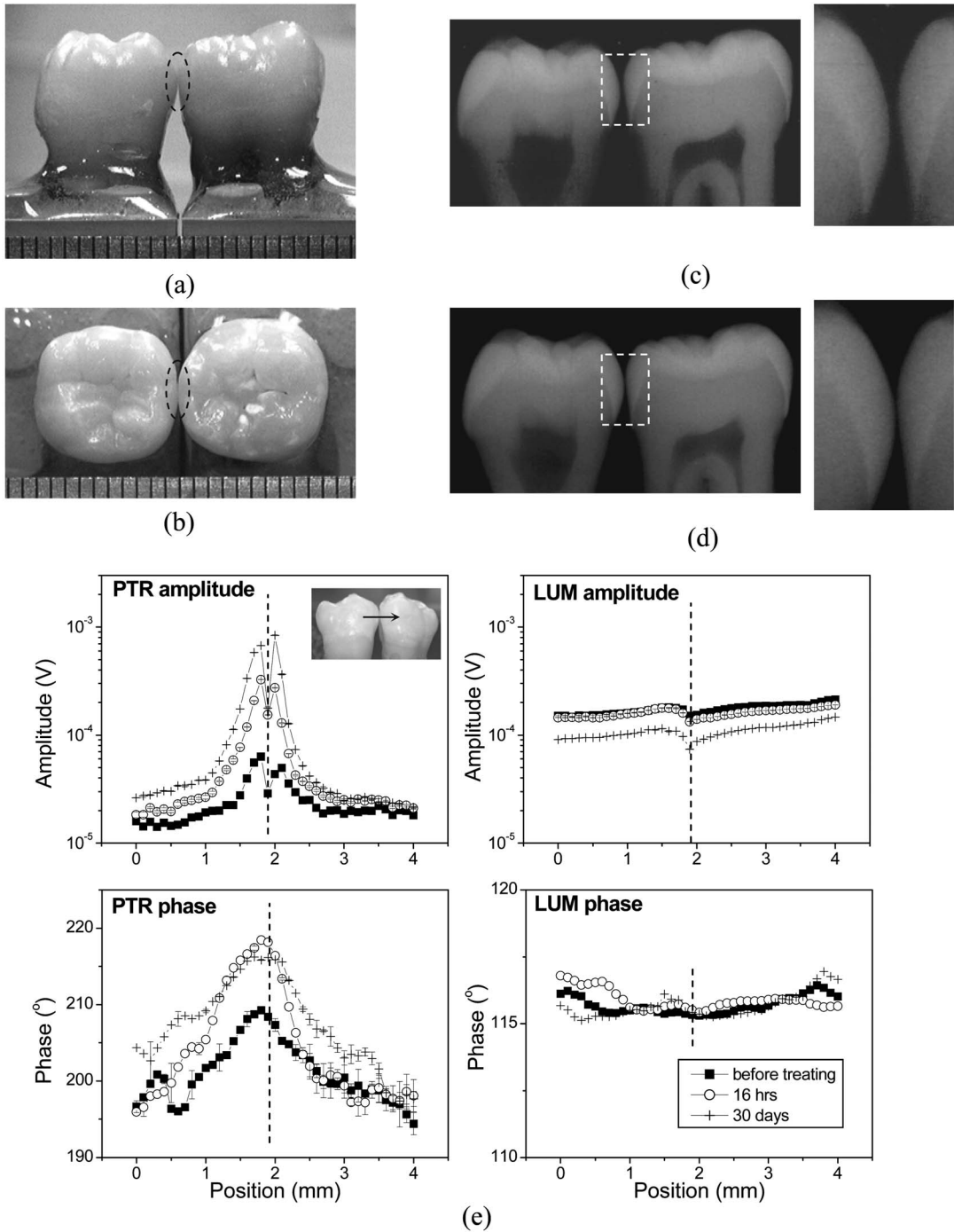
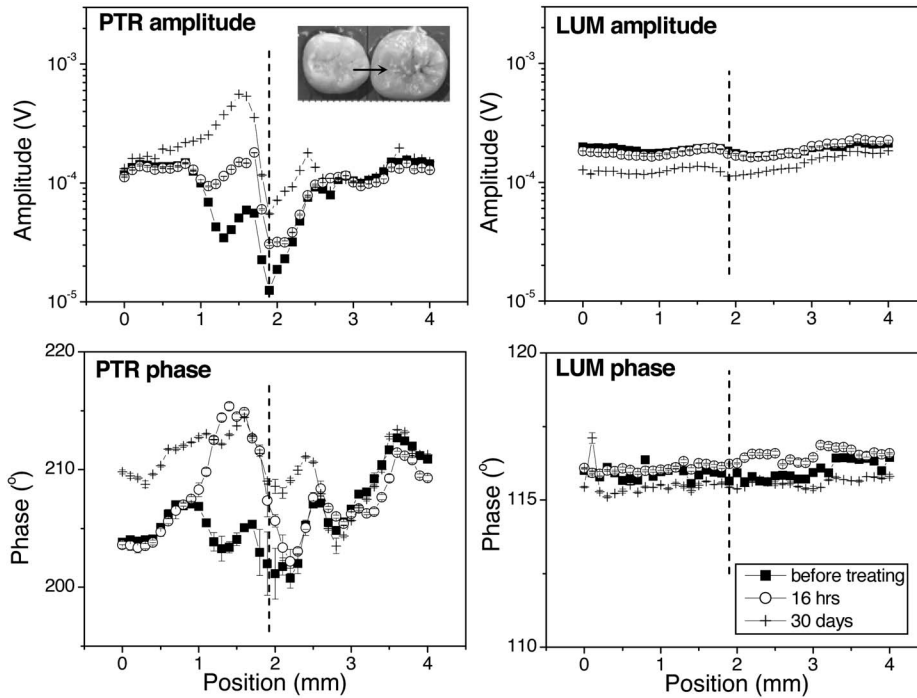


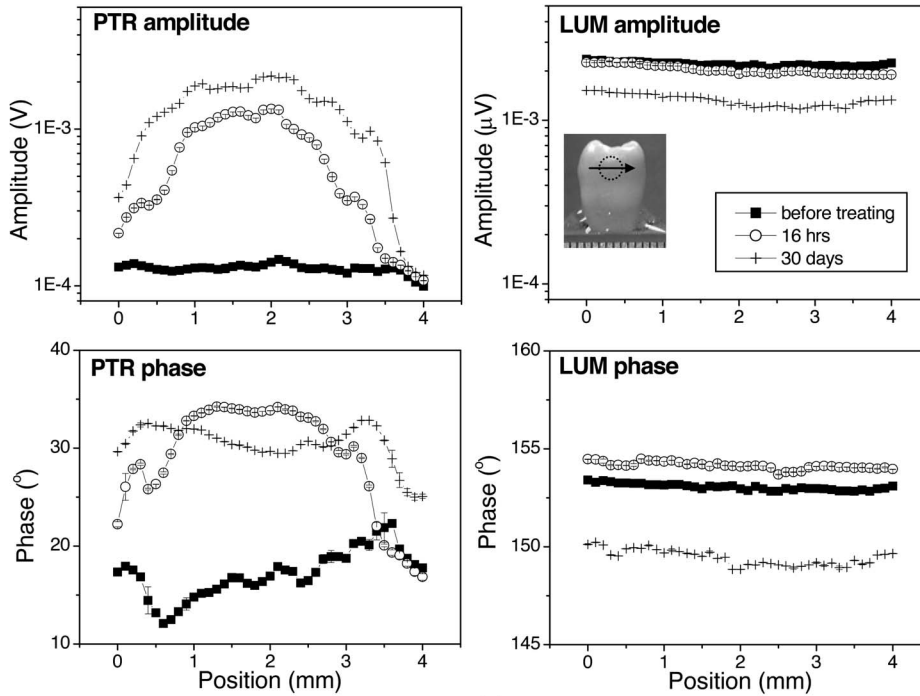
Fig. 7 Interproximal sample with demineralized lesion created by the buffer solution: (a) side view and (b) top view of the tooth pair; (c) radiograph of the tooth pair before treatment and a magnified view of the contact spot on the right; (d) radiograph of the tooth pair after treatment for 30 days on both contact spots and a magnified view of the contact spot on the right; (e) interproximal scan results on the buccal surfaces at 30 Hz; (f) interproximal scan results on the occlusal surfaces at 30 Hz; (g) line scan results on a single tooth across the treated area, and (h) typical PTR/LUM signal kinetics versus treatment time at 5, 50, and 500 Hz for a sequentially treated single tooth.

of the enamel affecting the entire surface. In these experiments, both buccal and occlusal scans exhibit similar levels of sensitivity to the creation of the demineralized lesions. Figure 7(g) shows a typical line scan with the incident laser beam normal to the demineralized surface. The decrease was more pronounced after the 30-day treatment. After the 16-h treat-

ment, PTR amplitude and phase clearly increased, especially at the center of the treated area (0.5 to 3.5 mm), with minimal or no shift of the signal from the untreated region. Figure 7(h) shows signal changes with treatment time at 5, 50, and 500 Hz. These data were extracted from frequency scans fol-



(f)



(g)

Fig. 7 (Continued).

lowing each treatment time. PTR amplitude and phase increased quite steeply after the first 16-h treatment; beyond that, they increased marginally until 80 h of treatment. Both signal channels decreased somewhat after 100 h, remaining essentially flat thereafter. The higher the frequency, the steeper the decrease observed after 80 h in both PTR amplitude and phase. It is noted that our LUM signal amplitudes

also exhibited the steepest rate of descent at early demineralizing times, consistent with the rate of steepest ascent of the PTR signals. All the samples exhibited this behavior, which may be due to partial saturation interaction between the solution and the enamel or partial remineralization of the enamel surface over time. Overall, the PTR signals tend to increase with longer treatment time, while the LUM signals tend to

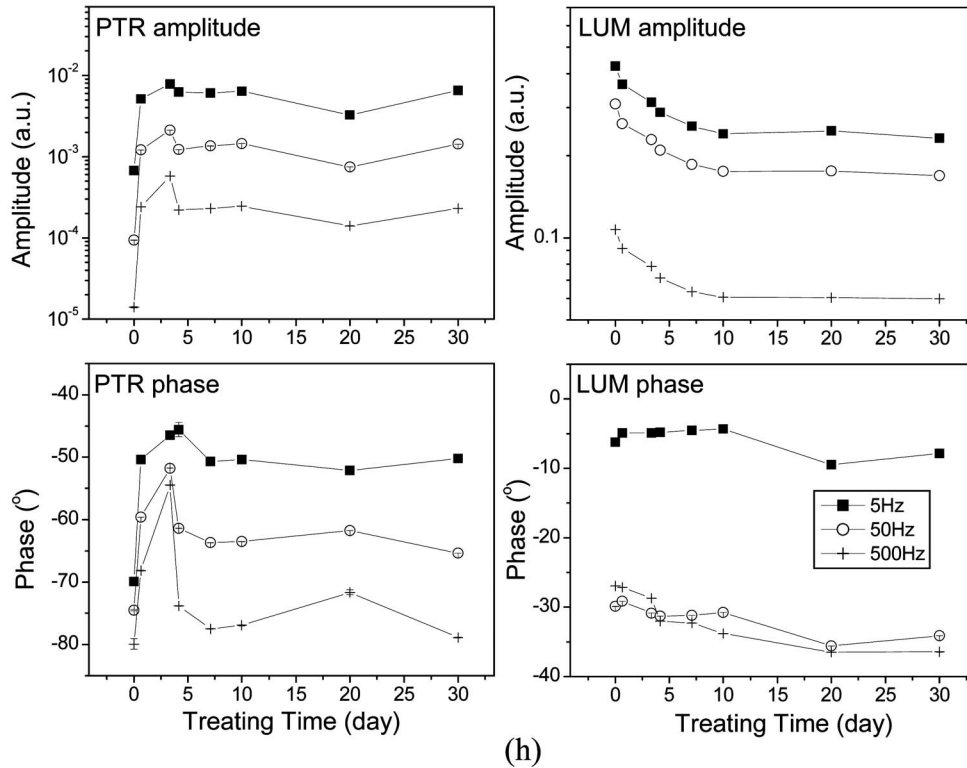


Fig. 7 (Continued).

decrease slightly. The radiographs before treatment [Fig. 7(c)] and after the full 30-day treatment [Fig. 7(d)] show no differences.

Another seven pairs of teeth were treated with the saturated buffer solution and examined in a similar manner except for the treatment time. Each pair was treated over different times; for example, the first pair was treated for only 6 h and the last pair was treated for 30 days. The purpose of doing so was to see if TMR and/or  $\mu$ -CT could resolve different levels of mineral loss (density changes) and determine lesion depths. The PTR signals, shown in Figs. 8(a) and 8(b) at 5 and 500 Hz, respectively, increased with treatment time, while the LUM signals slightly decreased, consistent with trends in Fig. 7. The observed LUM amplitude decreases with increasing degree of demineralization are also consistent with earlier findings<sup>26</sup> in which quantitative light-induced fluorescence (QLF), a form of dc luminescence, was used.

After all the measurements,  $\mu$ -CT, TMR, and SEM were used to measure the mineral loss ( $\mu$ -CT and TMR) and the lesion depth (TMR) as well as to obtain high-resolution cross-sectional images around the treatment location (SEM). Figures 9(a) and 9(b) show the  $\mu$ -CT and TMR images, respectively, for one of the 30-day treated samples. Both the  $\mu$ -CT and TMR showed the images that were produced to have the characteristics of eroded enamel lesion, i.e., a crater and a certain depth of demineralization at the base of the lesion. Although the demineralization at the base of the lesion is not easily recognizable in either image, both the mineral concentration measurement by  $\mu$ -CT and the mineral loss measurement by TMR indicated a significant loss of mineral in this area compared to the sound tissue area. However, the top-

down SEM images on an untreated enamel surface in Fig. 9(c) and a treated surface in Fig. 9(d) show difference in mineralization between the sound and demineralized tissue, with disappearance of the honeycomb shape (enamel prisms) after treatment. TMR showed the mineral loss and the lesion depth to be in the range of 110.8 to 905.4 vol%  $\mu$ m and 5.9 to 31.0  $\mu$ m, respectively, while the  $\mu$ -CT indicated a mineral loss of 0.36 to 1.6  $\text{cm}^{-1}$ . The best correlation between these two methods and the PTR/LUM signals was obtained between the PTR amplitude differences versus mineral loss with  $\mu$ -CT, which yields a correlation coefficient of 0.71, as shown in Fig. 10. It was hard to find a relationship between mineral loss (or lesion depth) and treatment time for both TMR (correlation coefficient: 0.44) and  $\mu$ -CT (correlation coefficient: 0.41). This is in part due to the small number of samples, since for treatments up to 10 days there were only 2 samples per treatment time. Another probable contributing factor is widely different demineralization rates from tooth to tooth. It was found that the mineral losses and the lesion depths after the full 30-day treatment were too widely distributed to yield meaningful mean and standard deviation values. This wide distribution of mineral loss from teeth has also been reported by de Josselin de Jong et al.<sup>27</sup> and supports large variations in demineralization rates across the investigated sample. On the other hand, Eggertsson et al.<sup>11</sup> mentioned that creating chemical caries lesions on natural surfaces of extracted teeth had proved to be quite difficult, which might be related to either high concentration of fluoride in the superficial enamel layers or to organic debris tenuously adhering to the tooth. This implies that extracted human teeth may have widely different surface mechanical and chemical properties with the result

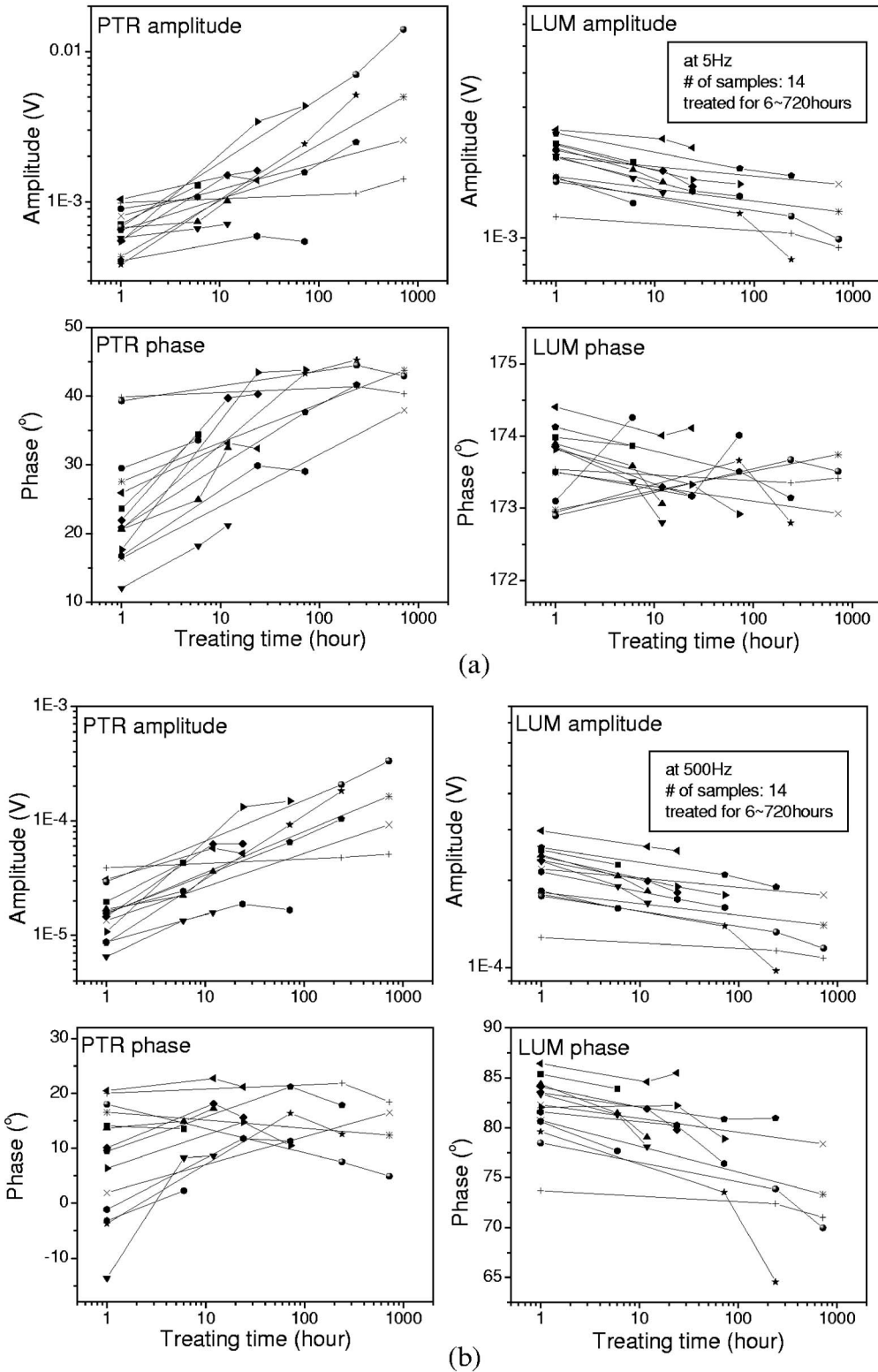
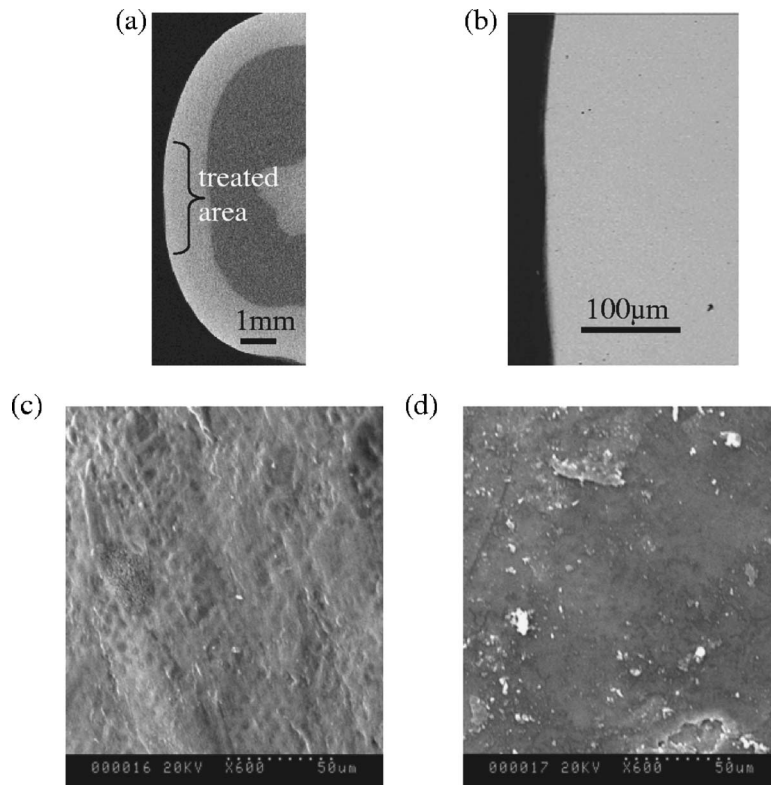


Fig. 8 PTR/LUM signals versus treatment time for multiple samples with treatment time intervals from 6 h to 30 days at (a) 5 and at (b) 500 Hz.

that some can be easily treated chemically while others cannot. Consistent with these observations, it follows that optical and thermophysical properties of dental enamel would also be expected to vary widely among healthy teeth. The correlation coefficient between the TMR and the  $\mu$ -CT data shown in

Fig. 11 is only 0.37. This indicates that one or the other method is less sensitive to changes incurred by our treatments. In view of the good correlation of PTR with  $\mu$ -CT results shown in Fig. 10, and considering the well-known ability of



**Fig. 9** (a)  $\mu$ -CT cross-sectional image of a 30-day-treated sample, (b) TMR cross-sectional image of a 30-day-treated sample, (c) typical SEM top-down image of an intact enamel surface, and (d) SEM top-down image of a 30-day-treated sample.

$\mu$ -CT to monitor mineral loss depthwise in enamel,<sup>24</sup> it can be concluded that PTR/LUM is capable of monitoring early demineralization in enamel. It remains largely unclear why TMR results do not agree with those obtained by  $\mu$ -CT; it is, however, quite likely that the reason is related to the absence of reliable TMR mineral loss calibration curves for our measurements of very early demineralization. On the contrary, adequate  $\mu$ -CT calibration data for early demineralization were available.

#### 4 Conclusions

Frequency domain PTR (FD-PTR) was assessed to be capable of detecting artificial interproximal mechanical defects and demineralized lesions in human teeth. Mechanical holes and phosphoric acid etched enamel surfaces in the interproximal region, which are too small to appear in dental radiographs, exhibited clear differences in PTR signals. Modulated luminescence was also measured simultaneously, but it exhibited a lower degree of contrast to these interproximal lesions and stronger dependency than PTR on factors affecting wider enamel regions than the treated interproximal spots, possibly

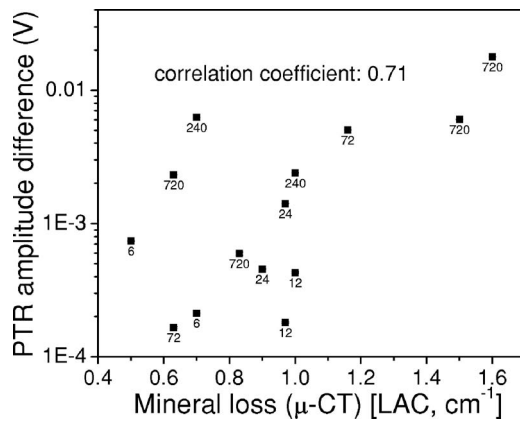


**Fig. 10** Correlation between PTR amplitude differences and  $\mu$ -CT mineral loss measurements. The numbers below each datum represent hours of demineralization.

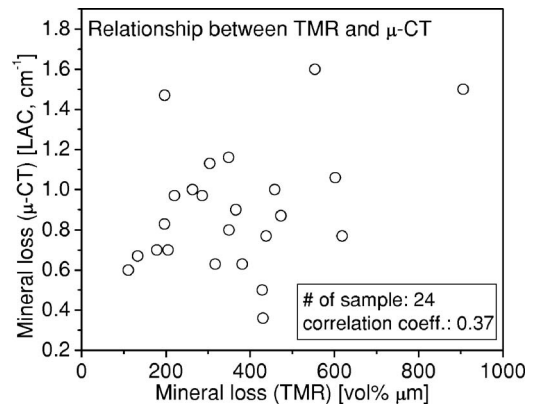


**Fig. 11** Correlation of mineral losses measured by TMR and  $\mu$ -CT on the same set of samples.

factors such as the hydration state of the surface. The demineralized interproximal lesions created by a saturated acidic buffer after continuous exposure from 6 h to 30 days were examined by PTR and LUM. The PTR amplitude increased more than 300% after treatment with the acidic buffer for 80 hours and the PTR phase also changed 5 to 13 deg at 30 Hz. Dental bitewing radiographs were also taken to determine whether x-rays could identify these demineralized lesions as well, but they showed no sign of lesion even for samples treated for 30 days. After completing all the experiments,  $\mu$ -CT, TMR, and SEM analyses were performed to compare and potentially correlate the PTR signals to depths of lesions and density changes. Only SEM images of the treated surface showed slight changes, while cross-sectional images showed no visible lesions. The mineral losses computed by TMR and the measured TMR lesion depths did not show clear correlation with total treatment time. The cross-correlation coefficient between the  $\mu$ -CT and the TMR data was only 0.37, a very low correlation, which seems to be due to the extremely small changes caused by the buffer solution treatment, absence of reliable calibration data for TMR in the ultrashallow lesion range below 40  $\mu$ m and possibly relative differences in detectivity of these techniques of our artificial lesions. PTR results yielded good correlation with independent  $\mu$ -CT mineral loss measurements. By virtue of its validation by  $\mu$ -CT measurements, a technique that is well-known for its ability to monitor early demineralization lesions in dental enamel, PTR has been shown to have the potential to be a reliable noninvasive tool for the detection of early interproximal demineralized lesions, which cannot be detected by conventional dental x-rays.

### Acknowledgment

The support of Materials and Manufacturing Ontario (MMO) with a Collaborative Contract and of Four Cell Consulting is gratefully acknowledged.

### References

- G. N. Jenkins, "Recent changes in dental caries," *Br. Med. J.* **291**, 1297–1298 (1985).
- D. Ricketts, E. Kidd, K. Weerheijm, and H. de Soet, "Hidden caries: what is it? Does it exist? Does it matter?" *Int. Dent. J.* **47**, 259–265 (1997).
- D. McComb and L. E. Tam, "Diagnosis of occlusal caries: part I. Conventional methods," *J. Can. Dent. Assoc.* **67**, 454–457 (2001).
- K. J. Anusavice, "Need for early detection of caries lesions," in *A United States Perspective in Early Detection of Dental Caries II, Proc. 4th Annual Indiana Conf.*, G. Stookey, Ed., pp. 13–30 (2001).
- R. Hibst and K. Konig, "Device for detecting dental caries," U.S. Patent No. 5,306,144 (1994).
- R. Hibst, R. Gall, and M. Klafke, "Device for the recognition of caries, plaque or bacterial infection on teeth," U.S. Patent No. 6,024,562 (2000).
- H. M. Alwas-Danowska, A. J. M. Plasschaert, S. Suliborski, and E. H. Verdonschot, "Reliability and validity issues of laser fluorescence measurements in occlusal caries diagnosis," *J. Dent.* **30**, 129–134 (2002).
- A. Lussi, S. Imwinkelried, N. B. Pitts, C. Longbottom, and E. Reich, "Performance and reproducibility of a laser fluorescence system for detection of occlusal caries in vitro," *Caries Res.* **33**, 261–266 (1999).
- X.-Q. Shi, U. Welander, and B. Angmar-Månsson, "Occlusal caries detection with KaVo DIAGNOdent and radiography: an in vitro comparison," *Caries Res.* **34**, 151–158 (2000).
- X.-Q. Shi, S. Tranæus, and B. Angmar-Månsson, "Comparison of QLF and DIAGNOdent for quantification of smooth surface caries," *Caries Res.* **35**, 21–26 (2001).
- H. Eggertsson, M. Analoui, M. H. van der Veen, C. González-Cabezas, G. J. Eckert, and G. K. Stookey, "Detection of early interproximal caries in vitro using laser fluorescence, dye-enhanced laser fluorescence and direct visual examination," *Caries Res.* **33**, 227–233 (1999).
- W. Buchalla, A. M. Lennon, M. H. van der Veen, and G. K. Stookey, "Optimal camera and illumination angulations for detection of interproximal caries using quantitative light-induced fluorescence," *Caries Res.* **36**, 320–326 (2002).
- A. Lussi, A. Hack, I. Hug, H. Heckenberger, B. Megert, and H. Stich, "Detection of approximal caries with a new laser fluorescence device," *Caries Res.* **40**, 97–103 (2006).
- J. D. Baders and D. A. Shugars, "A systematic review of the performance of a laser fluorescence device for detecting caries," *J. Am. Dent. Assoc.* **135**, 1413–1426 (2004).
- A. Mandelis, L. Nicolaidis, C. Feng, and S. H. Abrams, "Novel dental depth profilometric imaging using simultaneous frequency-domain infrared photothermal radiometry and laser luminescence," *Proc. SPIE* **3916**, 130–137 (2000).
- L. Nicolaidis, A. Mandelis, and S. H. Abrams, "Novel dental dynamic depth profilometric imaging using simultaneous frequency-domain infrared photothermal radiometry and laser luminescence," *J. Biomed. Opt.* **5**, 31–39 (2000).
- A. Mandelis, "Review of progress in theoretical, experimental, and computational investigations in turbid tissue phantoms and human teeth using laser infrared photothermal radiometry," *Proc. SPIE* **4710**, 373–383 (2002).
- R. J. Jeon, C. Han, A. Mandelis, V. Sanchez, and S. H. Abrams, "Diagnosis of pit and fissure caries using frequency-domain infrared photothermal radiometry and modulated laser luminescence," *Caries Res.* **38**, 497–513 (2004).
- R. J. Jeon, A. Mandelis, V. Sanchez, and S. H. Abrams, "Non-intrusive, non-contacting frequency-domain photothermal radiometry and luminescence depth profilometry of carious and artificial subsurface lesions in human teeth," *J. Biomed. Opt.* **9**, 804–819 (2004).
- L. Nicolaidis, C. Feng, A. Mandelis, and S. H. Abrams, "Quantitative dental measurements by use of simultaneous frequency-domain laser infrared photothermal radiometry and luminescence," *Appl. Opt.* **41**(4), 768–777 (2002).
- J. M. ten Cate and P. P. E. Duijsters, "Influence of fluoride in solution on tooth demineralization, I. Chemical data," *Caries Res.* **17**, 193–199 (1983).
- B. T. Amaechi, S. M. Higham, and W. M. Edgar, "Factors affecting the development of carious lesions in bovine teeth in vitro," *Arch. Oral Biol.* **43**, 619–628 (1998).
- S. E. P. Dowker, J. C. Elliot, G. R. Davis, R. M. Wilson, and P. Cloetens, "Synchrotron x-ray microtomographic investigation of mineral concentration at micrometer scale in sound and carious enamel," *Caries Res.* **38**, 514–522 (2004).
- E. de Josselin de Jong, J. J. ten Bosch, and J. Noordman, "Optimised microcomputer guided quantitative microradiography on dental mineralized tissue slices," *Phys. Med. Biol.* **32**, 887–899 (1987).
- B. T. Amaechi, S. M. Higham, and W. M. Edgar, "Use of transverse microradiography to quantify mineral loss by erosion in bovine enamel," *Caries Res.* **32**, 351–356 (1998).
- B. T. Amaechi and S. M. Higham, "Quantitative light-induced fluorescence: a potential tool for general dental assessment," *J. Biomed. Opt.* **7**, 7–13 (2002).
- E. de Josselin de Jong, A. H. I. M. van der Linden, P. C. F. Borsboom, and J. J. ten Bosch, "Determination of mineral changes in human dental enamel by longitudinal microradiography and scanning optical monitoring and their correlation with chemical analysis," *Caries Res.* **22**, 153–159 (1988).